The effect of gear tooth surface quality on diagnostic capability

Ido Dadon[1], Niv Koren[1], Renata Klein[2] and Jacob Bortman[1]

[1]Pearlstone Center for Aeronautical Engineering Studies and Laboratory for Mechanical Health Monitoring, Department of Mechanical Engineering, Ben-Gurion University of the Negev
P.O. Box 653, Beer Sheva 8410501, Israel
dadoni@post.bgu.ac.il

[2]R.K. Diagnostics
P.O. Box 101, Gilon, D.N. Misgav 20103, Israel

Abstract

A real gear transmission contains geometrical errors, which directly influence the vibration signature. The geometric errors may restrict the ability of fault diagnostics. To better understand the limits of fault detection in the presence of different levels of gear imperfection, a need arose for the modelling of geometric errors.
This study focuses on profile deviation as part of the geometric errors deriving from manufacturing errors. The profile deviation is defined in respect to the ideal profile. As the manufacturing process is more precise, the quality of the gears increases and, accordingly, the tooth profile errors are minimized.
The effect of tooth profile errors on fault detection capability is studied. A validated dynamic model that simulates the vibrations of gears with different types and sizes of faults was utilized.
This paper proposes an expression for the representation of the tooth profile errors that takes into consideration the irregularity of the gear teeth representing a realistic system. It is shown that low profile precision grade reduces the ability to detect faults. It is demonstrated that the model predicts correctly the detectable fault severity for a given profile precision grade. Moreover, the model estimates the distribution of results generated by profile errors, allowing robustness analysis of diagnostics procedures.

1 Introduction

The vibration signal of a real gear transmission is affected by unintentional profile errors, which are caused by the manufacturing process. The amount of profile errors depends on the manufacturing precision grade. To better understand the effects of profile errors on diagnostic capability, a description of the actual tooth surface is required.

Several studies in the field of modelling of gears imperfection have been made. However, the influences of the gear tooth precision grade on the fault detection capability are not studied yet. Fernández et al. [1] presented an analytical formulation of profile deviations such as tip reliefs and undesired profile errors. They assumed that deviations from the theoretical profile due to the manufacturing process or wear are not large enough to affect the overall flexibility of the tooth or the normal direction of the contact force. Thus, the inclusion of this phenomenon only affects the calculation of the distance between potential contact points. The formulation of the profile errors was carried out following the approach proposed by Mucchi et al. [2], adopting a sinusoidal shape as a function of the radius of the contact point. The profile errors were considered identical for all teeth. However, this assumption is weak since the error values are random for each tooth, hence it will significantly influence the dynamic behaviour. In addition, their dynamic simulations were not verified with experiments.

In this study, we examine the sensitivity of gear vibrations with respect to different gear teeth surface qualities and their effects on fault detection capability. A dynamic model of gear systems is used in this study. A modification to the analytical formulation of the profile error is proposed. Here, we consider different error

profiles for each tooth of a gear wheel. The simulations are qualitatively compared with experiments of different precision grades of spur gears in the presence of local faults.

The work is organized in the following manner. The dynamic model of a gear transmission and the formulation of tooth profile errors are described in chapter two. The experimental tests are detailed in the third chapter. The data analysis process of the experimental and simulated signals is described in the fourth chapter. In addition, a comparison between the experimental and simulation (model) results is presented. Finally, a short summary concludes our work.

2 Theoretical model

A dynamic model for prediction of gear system vibrations was used in order to examine the effects of gear tooth profile errors on the diagnostic capability. The following chapter describes the dynamic model, specifically the modelling of the tooth profile errors.

2.1 Gear system dynamics

A multi-degree of freedom dynamic model of a loaded gear system was developed [3]. An illustration of the gear system modelling approach is presented in Figure 1. The interaction between a gear pair along the pressure line is modelled using:

- A linear spring with variable stiffness k_e. The stiffness value depends on the angular position of the gears.
- Displacement b is half of the nominal size of the clearance between meshing teeth (backlash). The contact between teeth meshing depends on the relative displacement of the gear pair in relation to the backlash value.
- An error forcing function, $e(t)$, defines the geometric error of the gear pair. The geometric errors usually represent the installation errors and profile deviations.

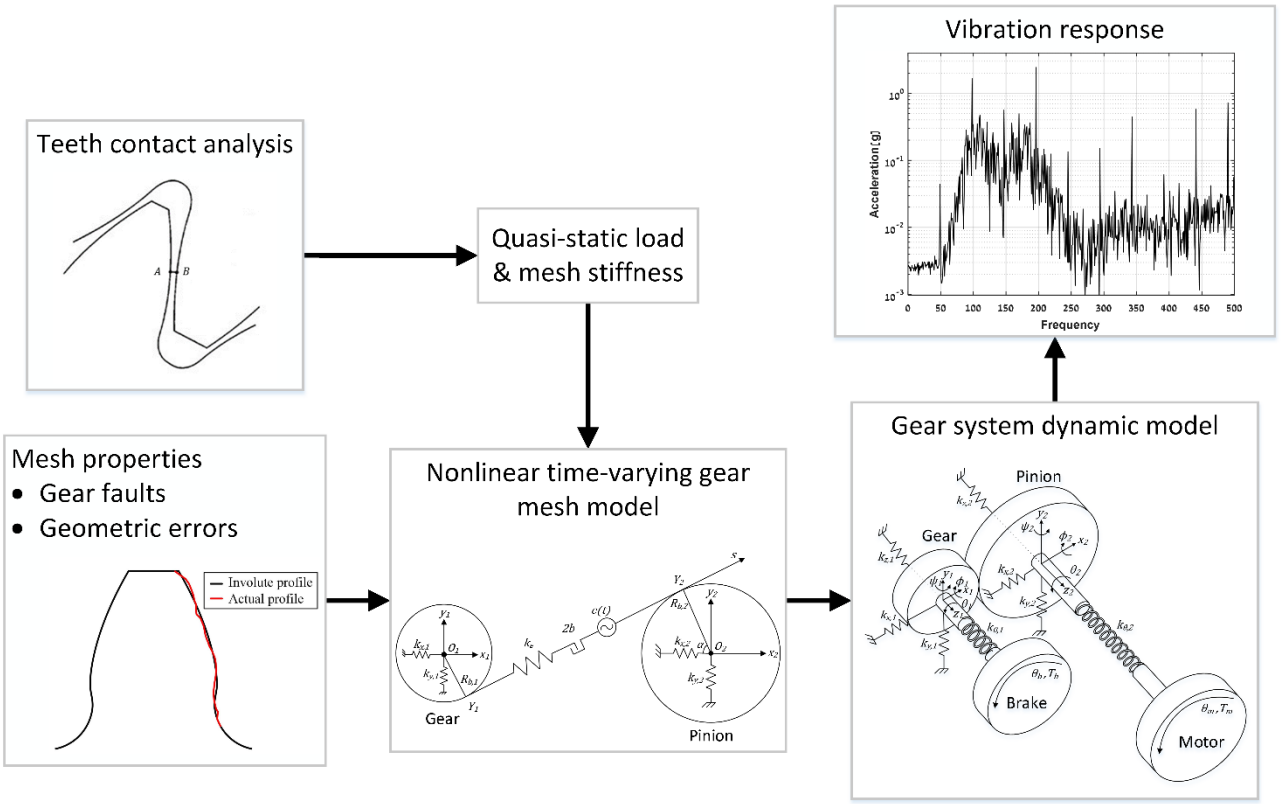

Figure 1: Gear system modelling approach.

The teeth contact analysis is performed in order to estimate the gear mesh stiffness. The stiffness is determined by an analytical expression, which takes into account the strain energy, Herzian contact and gear-body induced tooth deflection due to contact of teeth.

The mesh properties, such as gear faults and geometric error, are considered in the gear mesh model. The geometric error is given as a displacement-excitation function along the pressure line. Tooth profile errors, which are produced in the manufacturing process, are examined in this study (discussed in detail in chapter 2.2). Also, the gear mesh model enables to examine different type of faults, which are characterized by reduction of the gear mesh stiffness and by variation of the tooth profile.

The gear system dynamic model includes six degrees-of-freedom for each gear wheel, which are assumed to be rigid bodies. Also, the motor and the loading component (brake) are assumed to be rigid bodies with torsional degree-of-freedom. The two shafts are assumed to be of finite torsional stiffness and infinite bending stiffness. The shafts are supported by bearings, which are modelled by linear springs with constant stiffness. The damping expressions are determined from modal damping ratios of the structure. A constant input velocity (motor) and an external applied load (brake) are the boundary conditions of the problem. Two spur gear pairs were simulated for this study. The parameters of the gear system are given in Table 1.

	Set A		Set B	
	Pinion	Gear	Pinion	Gear
Tooth numbers	17	49	17	38
Transverse moment of inertia (kg m2)	$I_2 = 6.4\times10^{-5}$	$I_1 = 1.4\times10^{-3}$	$I_2 = 9.8\times10^{-5}$	$I_1 = 1.6\times10^{-3}$
Polar moment of inertia (kg m2)	$J_2 = 6.0\times10^{-5}$	$J_1 = 2.6\times10^{-3}$	$J_2 = 1.1\times10^{-4}$	$J_1 = 2.7\times10^{-3}$
Module (mm)	2.5		3	
Tooth width (mm)	15		15	
Pressure angle	20°		20°	
Young modulus (N/m2)	210×10^9		210×10^9	
Poisson's ratio	0.3		0.3	
Bearing stiffnesses (N/m)	$k_{x,j} = k_{y,j} = k_{z,j} = 1.9\times10^8$ (j=1,2)			
Shafts' torsional stiffnesses (N m/rd)	$k_{\theta,1} = 1.9\times10^3$, $k_{\theta,2} = 7.9\times10^3$			
Modal damping ratios	$\zeta_n = 0.05$ (for all modes)			
Motor speed (RPS)	40			
Brake torque (N m)	10			

Table 1: Parameters of the gear system.

For each gear pair, tooth face faults of five different levels of severity were simulated on a single tooth in the driven gear. The geometry of the faults is presented in Figure 2. All faults were implemented across the entire tooth width. Severity was set by increasing the faults diameter (d = 1.5, 2.5, 3, 3.5, 4 [mm]). This type of faults are characterized by local alteration of the involute profile along the contact area. Meshing of a faulty tooth will cause displacement error, alteration of the pressure angle and reduction of the gear mesh stiffness, since there will be no contact between two involute profile at that moment. Figure 3(a) presents the displacement error due to the first three faults (for clarity) over the cycle of the 'Out' shaft. The displacement error occurs one time per rotation of the driven gear. The magnitude and duration of the response increase as function of the faults diameter. Figure 3(b) presents the pressure angle alteration due to the fault. The nominal angle value is 20° while sharp angle variations are visible at the interaction with the fault as a result of the direction change of the contact force. The magnitude of the pressure angle deviation from the nominal value increases as function of the faults diameter. The vibration response due to the reduction of the gear mesh stiffness, caused by the tooth face fault, was found to be negligible compared to the other effects of the fault (displacement error and pressure angle alteration).

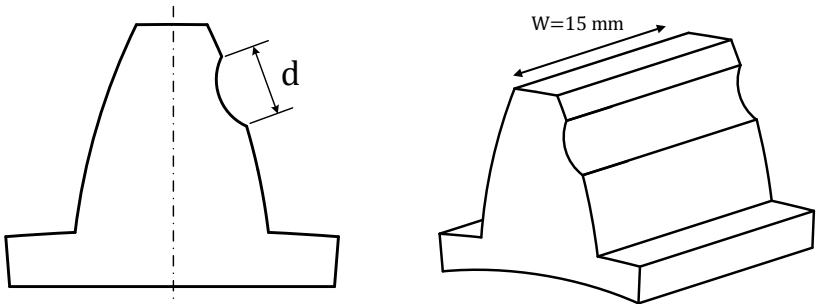

Figure 2: Tooth face fault geometric measurements.

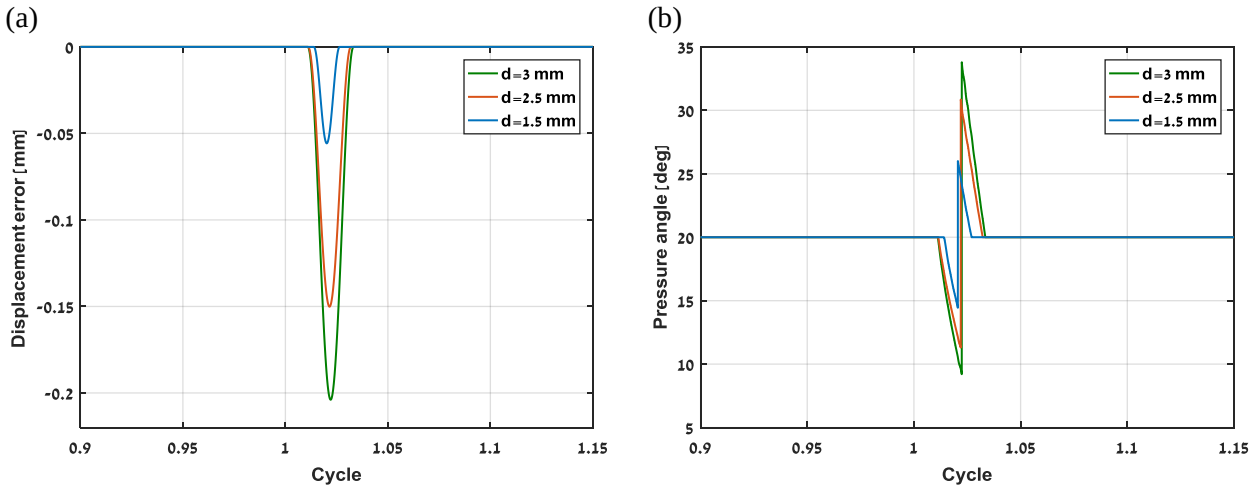

Figure 3: Dynamic characteristics of tooth face faults. (a) displacement error; (b) pressure angle.

2.2 Formulation of the profile deviation

A description of the actual tooth profile is required in order to examine the influences of the gear tooth precision grade on the fault detection capability. In this work, tooth profile errors are simulated in the gear mesh model. It is given as a displacement-excitation function along the pressure line.

The tooth profile error is defined as the deviation of the actual tooth profile from the ideal involute profile. The magnitude of the profile error depends on the gear precision grade. The following formulation simulates the tooth profile error:

$$e_{\mathrm{p}}(s(t)) = f_{\mathrm{H}\alpha}\frac{(s(t)-s_0)}{L} + \frac{f_{\mathrm{f}}}{2}\sin\left(2\pi n\frac{(s(t)-s_0)}{L}+\phi\right) + Err\cdot\mathrm{rand}(t) \tag{1}$$

This is a modified formulation, which is based on the work of Mucchi et al. [2]. It is expressed by composition of a linear and a sinusoidal term as a function of the coordinate s, which is the distance between a contact point P of the tooth profile and the tangent point to the base circle of the radius R_{b} (see Figure 4). The coordinate s can be expressed as a function of the radius of the contact point:

$$s(R_{\mathrm{p}}(t)) = R_{\mathrm{b}}\tan\left(\arccos\left(\frac{R_{\mathrm{b}}}{R_{\mathrm{p}}(t)}\right)\right) \tag{2}$$

$f_{\mathrm{H}\alpha}$ is the profile angle deviation and f_{f} is the profile form deviation, as shown in Figure 5. L is the functional length along the involute profile. It is obtained by subtraction of the upper and lower limits of coordinate s $(L = s_{\mathrm{f}} - s_0)$. n is the number of sinusoid cycles along the functional profile length and ϕ is the phase

component of the sinusoidal term. Here, we added an irregularity term with a uniform distribution, $\mathrm{rand}(t)$, in order to simulate different profile errors for each tooth describing a realistic profile. When simulating an identical profile error for all teeth, completely artificial periodic components will be generated in the vibration signal. Random values are drawn from a uniform distribution function, $\mathrm{rand}(t)$. *Err* is a value that quantifies the variation (standard deviation) of the uniform distribution. The irregularity term is represented by a uniform distribution, since the profile errors are assumed to be distributed equally between the manufacturing tolerances. We assume that the profile deviations are uniform along the tooth width. Also, we assume that the change of the gear mesh stiffness and the pressure angle as a result of profile errors are negligible. The general expression of the geometric error function is calculated by combining the profile deviations of each gear, as follows:

$$e(t) = e_{\mathrm{p-gear}}(t) + e_{\mathrm{p-pinion}}(t) \tag{3}$$

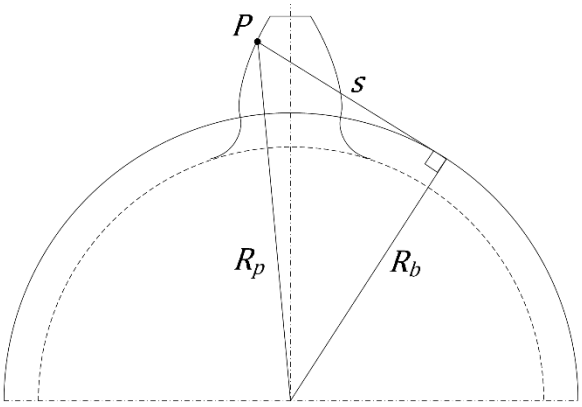

Figure 4: Parameters defining the profile errors [2].

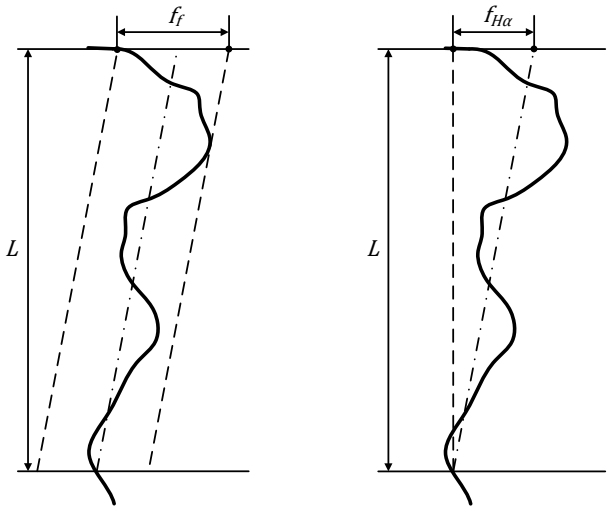

Figure 5: Tooth profile diagram [4].

The parameters of the profile errors were determined for two different gear tooth surface qualities: DIN 10 [5] (low quality) and DIN 7 (high quality). The profile errors are specified in Table 2. The parameters defining the profile errors ($f_{\mathrm{H}\alpha}$, f_{f} and n) are drawn for each gear tooth from a uniform distribution around the nominal error values (Table 2) with a variance coefficient of 10% of the nominal values. Figure 6 presents the simulated profile errors for both qualities over three adjacent teeth of the gear.

	Set A - DIN 10		Set B - DIN 7	
	Pinion	Gear	Pinion	Gear
Profile angle deviation $f_{H\alpha}$ (μm)	28	28	9	9
Profile from deviation f_f (μm)	36	36	11	11
Cycles n	2.5	3.5	2.5	3.5
Err (μm)	1	1	0.3	0.3

Table 2: Nominal parameters of the profiles errors.

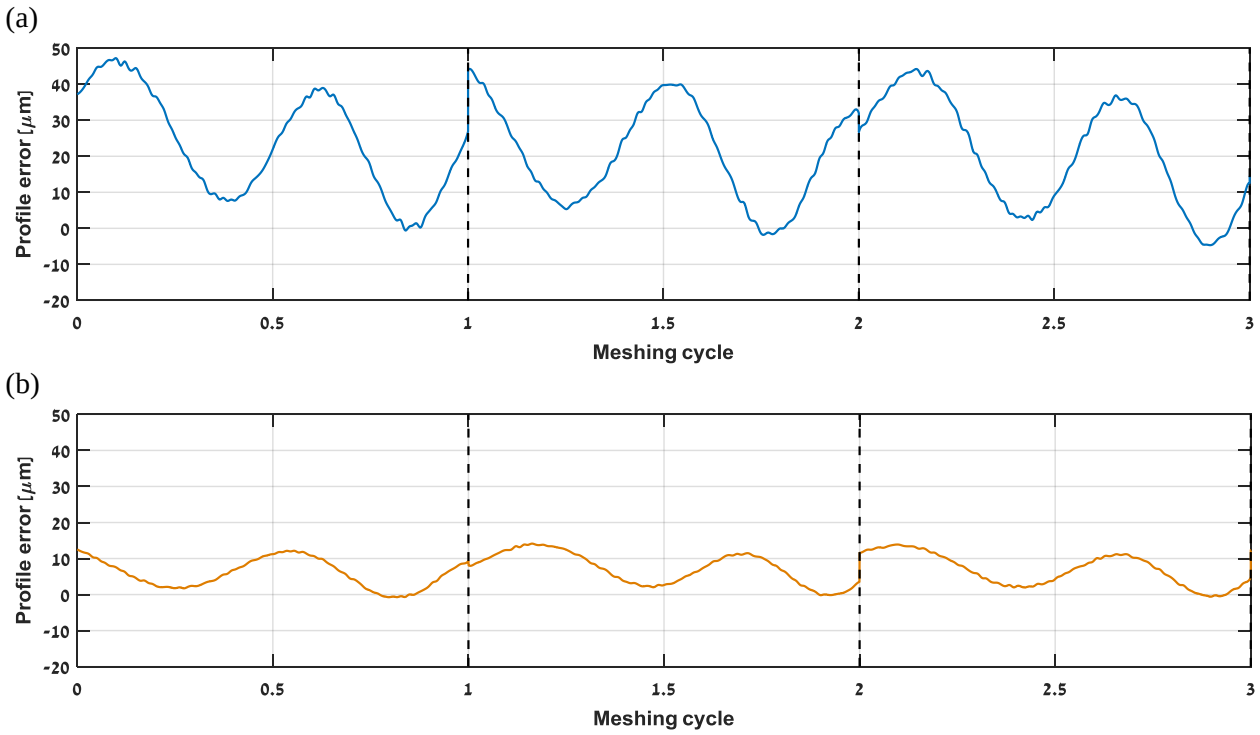

Figure 6: Simulated profile error over three adjacent teeth of the gear. (a) DIN 10; (b) DIN7.

3 Experimental setup

A spur gear transmission was used in this study. The transmission is driven by an asynchronous AC induction engine and loaded by a similar engine unit, modified as an alternator. A three-axial piezo-electric sensor was placed close to the transmission in order to measure the gear vibrations. A proximity sensor is used to record the rotating speed of the 'In' shaft. Furthermore, a torque meter was attached to the system, providing the loading torque measurement. The experimental system is described in Figure 7. The sampling rate in all tests was 25 [kSamples/sec]. All recordings were of 60 [sec] duration. Two spur gear sets of different tooth surface quality were examined, as described by Table 3. Photos of teeth illustrating the difference between the teeth surface qualities of the examined gear sets are presented in Figure 8.

	Transmission ratio	Module	Precision grade	RC
Set A: Low surface quality	49/17	2.5	AGMA 7 [4] / DIN 10	<30
Set B: High surface quality	38/17	3	AGMA 10 / DIN 7	50÷60

Table 3: Gear wheels parameter.

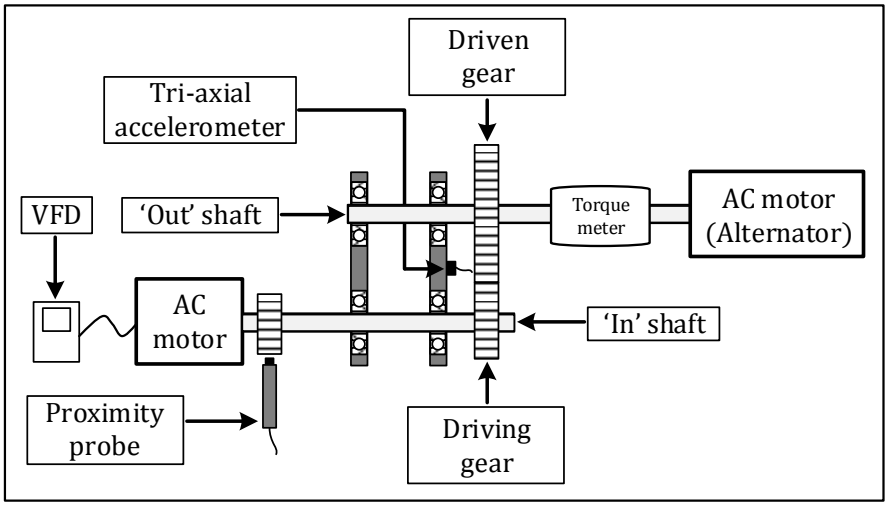

Figure 7: Experimental system scheme.

(a) (b)

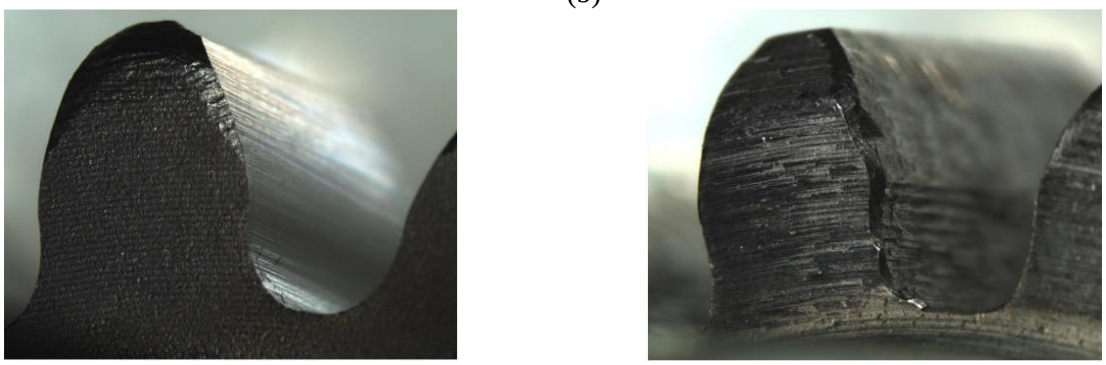

Figure 8: Different types of examined surfaces. (a) high quality (AGMA 10); (b) low quality (AGMA 7).

In both gear sets, a single tooth of the driven gear was milled in order to create a tooth face fault, simulating a spall across the entire contact area. The fault was seeded at five different levels of severity by changing the fault diameter. Figure 9 presents the first and fourth fault severities of both gear sets. Table 4 summarizes all the cases that were analysed in this study.

	Healthy	Fault 01 1.25÷1.50 [mm]	Fault 02 2.25÷2.50 [mm]	Fault 03 3.00÷3.25 [mm]	Fault 04 3.50÷3.75 [mm]	Fault 05 4.00÷4.25 [mm]
Set A: Low surface quality	LQH	LQF1	LQF2	LQF3	LQF4	LQF5
Set B: High surface quality	HQH	HQF1	HQF2	HQF3	HQF4	HQF5

Table 4: Different examined cases.

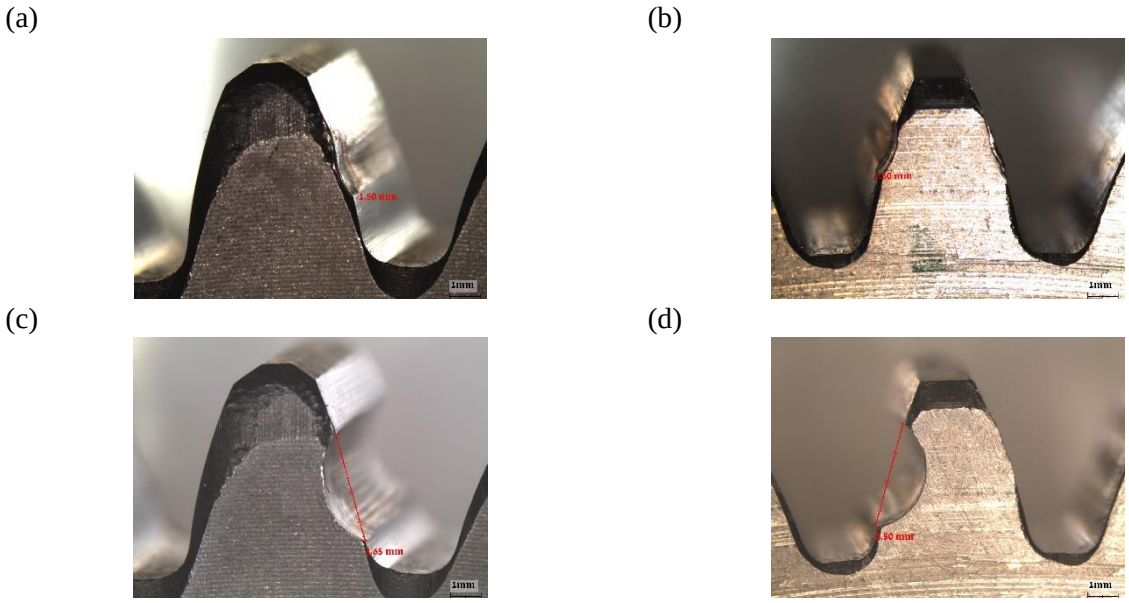

Figure 9: Examples of different sizes of local faults. (a) HQF1; (b) LQF1; (c) HQF4; (d) LQF4.

Every case was repeated six times in order to examine the experimental results distribution. The gear transmission has been partially dismantled between each repetition in order to obtain meshing of different teeth, simulating a six different gear pairs. The experiments were conducted at a rotational speed of 40 [RPS] ('In' shaft) and a loading torque of 10 [N m].

Figure 10 shows a scheme of the vibration signal components of a gear transmission. The measured vibration signal consists of three main components: the deterministic signal of the gears, which is derived from the meshing of teeth, the impulse due to the local fault and the excitation caused by effects of geometrical imperfections, in our case study, tooth profile errors. Convolution in the time domain of this signal with the impulse response representing the effects of the transmission path will give us the measured signal.

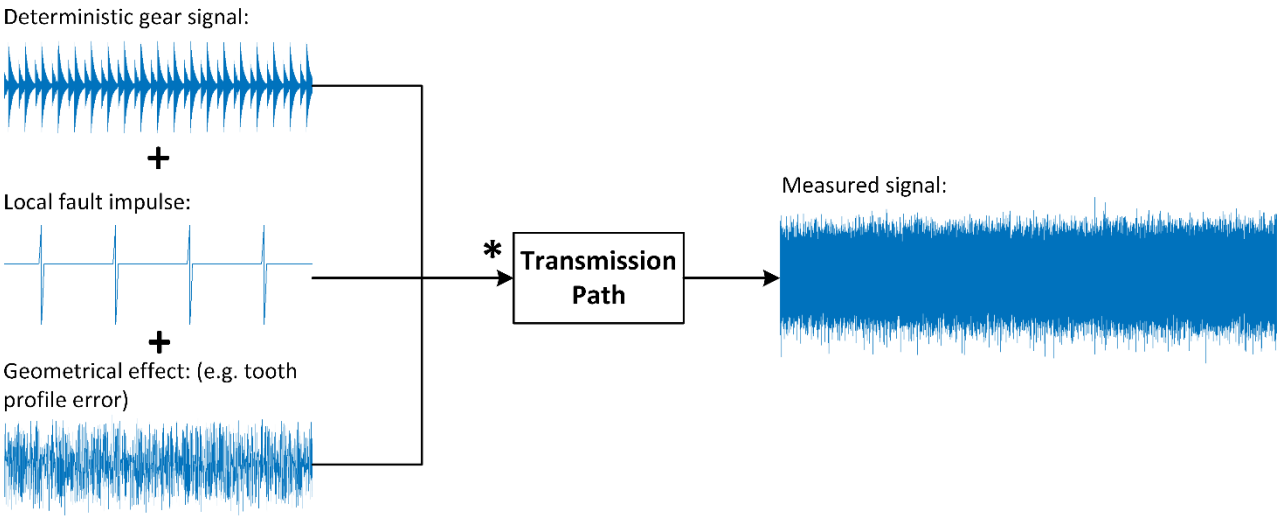

Figure 10: Vibration signal components of a gear transmission [6].

4 Model simulations and experimental results

The dynamic model was developed in order to facilitate the improvement of the diagnostics and prognostics of gears. The model is aimed to improve the physical understanding of effects of faults and to perform sensitivity analysis and assessment of detection capability in different configurations. In this study our focus is on validating the model and understanding the effect of gear tooth surface quality on fault detection

capability. Therefore, comparison of results of simulations and experiments will be discussed by the following chapter.

4.1 Data analysis

The experiments and dynamic simulations were conducted under the same operating conditions. Two gear sets of different precision grade were examined in the presence of local faults at five different levels of severity. An identical analysis for both experimental and simulation signals was performed in order to achieve a proper comparison. For simplification of the data analysis process, Figure 11 provides a general guidance scheme for each measurement/simulation.

Angular resampling is a common method for handling shaft velocity oscillations, which occur in all realistic revolving machinery. The resampling procedure synchronizes the time history according to a shaft rotating speed generating a signal in the cycle domain. Simulated signals do not undergo this part of the processing since a constant input velocity was defined. Separation of the vibrations excited by a certain gearwheel is obtained through the Synchronous Average (SA), the average of the resampled cycles. The SA task is to emphasize the vibrations synchronous to a specific shaft by removing the asynchronous vibrations caused by other elements such as other shafts, bearings, noise, etc., while keeping the entire relevant information about the gearwheels on the specific shaft. Two statistical moments, RMS and Kurtosis, are calculated from the SA signals. RMS reflects the vibration energy of the signal and Kurtosis provides a measure of the peakedness of the signal. The same analysis was performed on the difference and residual signals. The results obtained did not provide additional information and therefore are not presented.

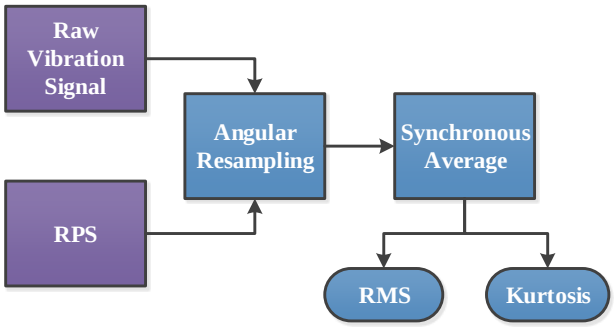

Figure 11: Data analysis flow chart of the procedure.

4.2 Results

The experiments included six repetitions of every case in order to obtain meshing of different teeth, simulating a different gear pair for each repetition. The model simulations were performed for six different gear pairs by drawing the teeth profile errors of the gear pair six times.

The following figures (Figure 12 and Figure 13) present a sample of the SA of all the test cases: ‘healthy’ and tooth face faults of five different levels of severity. Figure 12 displays the SA of the simulations for low and high tooth surface quality. Figure 13 displays the SA of the experiments for low and high tooth surface quality. These figures present the SA signals according to the ‘Out’ shaft (shaft carrying the faulty gear) for all the test cases. For convenience, one measurement/simulation from the six available is presented for each case.

It can be seen that in the simulations of the low-quality gear wheels, the fault of the first severity (LQF1) is unobservable. The impact generated by this fault is masked by the effects of the gear profile errors and therefore is undetectable. However, in the simulations of the high-quality gears the fault was obviously observable starting from the first fault severity (HQF1), as presented in Figure 12. A similar situation is obtained in the experimental signals, when for the high-quality gears the effects of the fault appear starting from the first fault severity (HQF1) and for the low-quality gears from the third fault severity (LQF3), as presented in Figure 13.

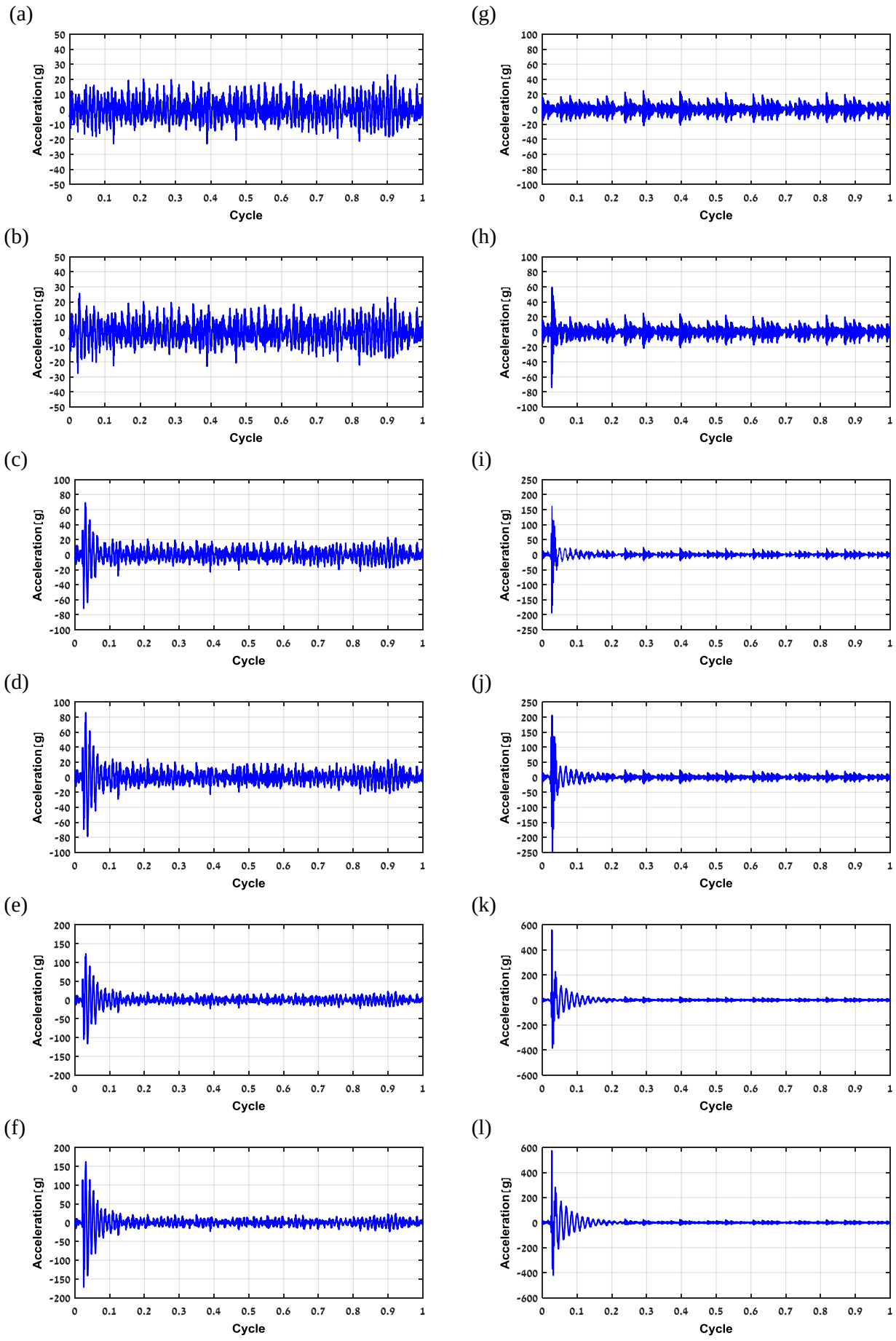

Figure 12: SA signal of the low and high surface quality - simulated results. (a) LQH; (b) LQF1; (c) LQF2; (d) LQF3; (e) LQF4; (f) LQF5; (g) HQH; (h) LQF1; (i) LQF2; (g) LQF3; (k) LQF4; (l) LQF5.

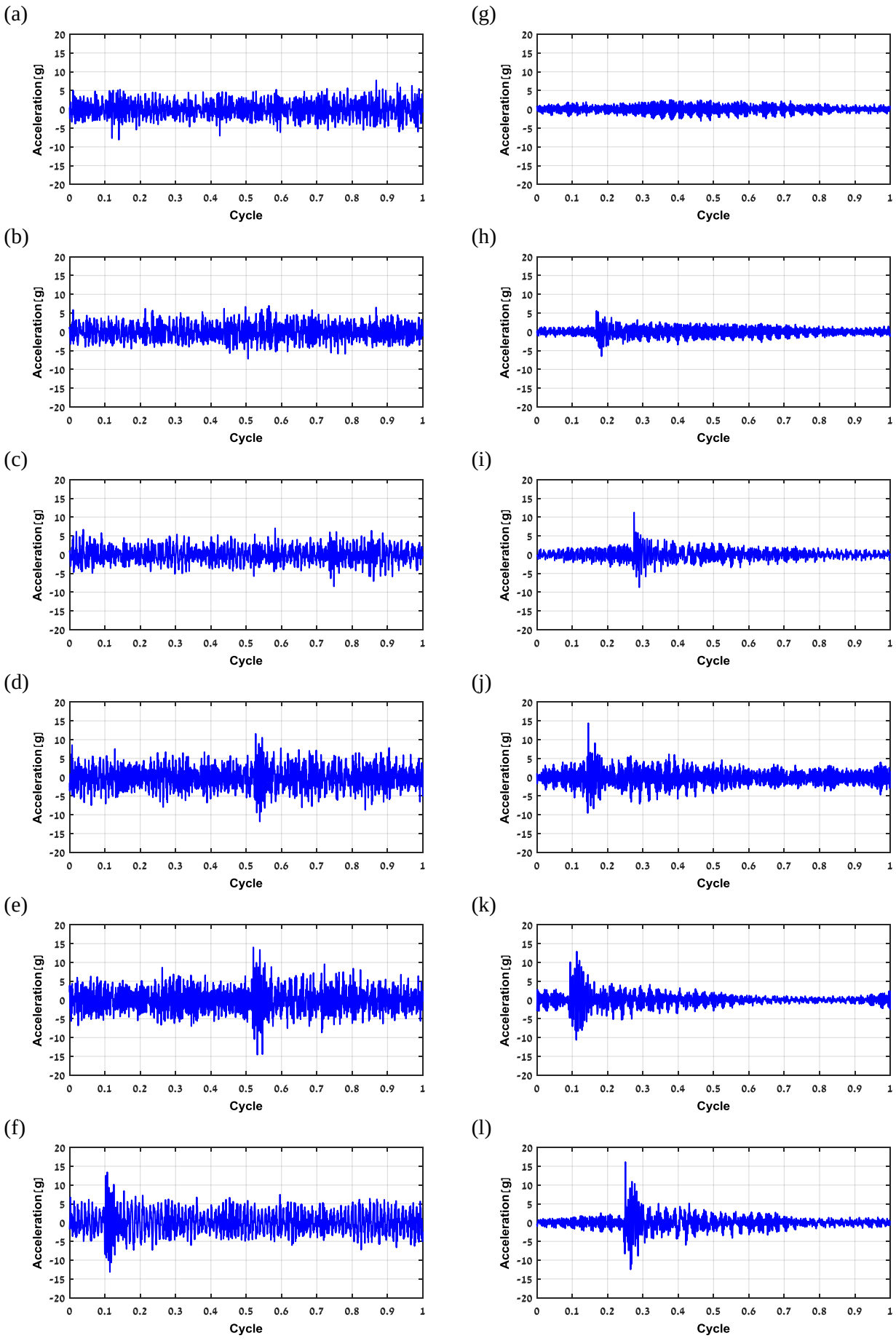

Figure 13: SA signal of the low and high surface quality - experimental results. (a) LQH; (b) LQF1; (c) LQF2; (d) LQF3; (e) LQF4; (f) LQF5; (g) HQH; (h) LQF1; (i) LQF2; (g) LQF3; (k) LQF4; (l) LQF5.

Figure 14 and Figure 15 summarize the results for all the six repetitions of each case (‘healthy’ and five different levels of severity). These figures present the RMS (y-axis) versus the Kurtosis (x-axis) of the SA signals for the ‘Out’ shaft. Figure 14 displays the simulation results of the low and high quality gears. Figure 15 displays the experimental results of the low and high quality gears.

The RMS values of the experimental signals are affected by the transmission path while the transmission path effects are not modelled, producing different ranges of values. RPS measurement errors, which subsequently cause energy leakage at high orders, are expected to decrease the peakedness of the signal affecting the Kurtosis. In the experimental results of the high quality teeth surface, the fault severities are not as well separated as are in the simulations due to the leakage at high orders. The simulated signals are not affected by the transmission and by the energy leakage, hence their statistical moments differ from the experiments.

It can be clearly seen, from the simulation results, that the fault detection capability depends on the teeth surface quality. A better separation between the healthy and faulty gears is obtained for the high-quality gears. The separation is expressed in both the RMS and Kurtosis, where the Kurtosis presents distinct results. The RMS presents more repeatable results and shows some sensitivity to the fault severity. For the high quality surface, a good separation between the fault severities can be observed. It should be noted that different teeth surface simulations generate scattered RMS and Kurtosis values. A similar picture of detectable faults is obtained in the experimental results, as can be observed in Figure 15.

It was shown that the model predicts correctly the detectable fault severity for a given teeth surface quality and that gears with high quality teeth surface allow detection of smaller faults. The model is a powerful tool for assessing diagnostics capabilities and their robustness in a real environment. The number of experiments that can be performed is always limited. The model can be used to extend the number of cases and to obtain a realistic distribution of results.

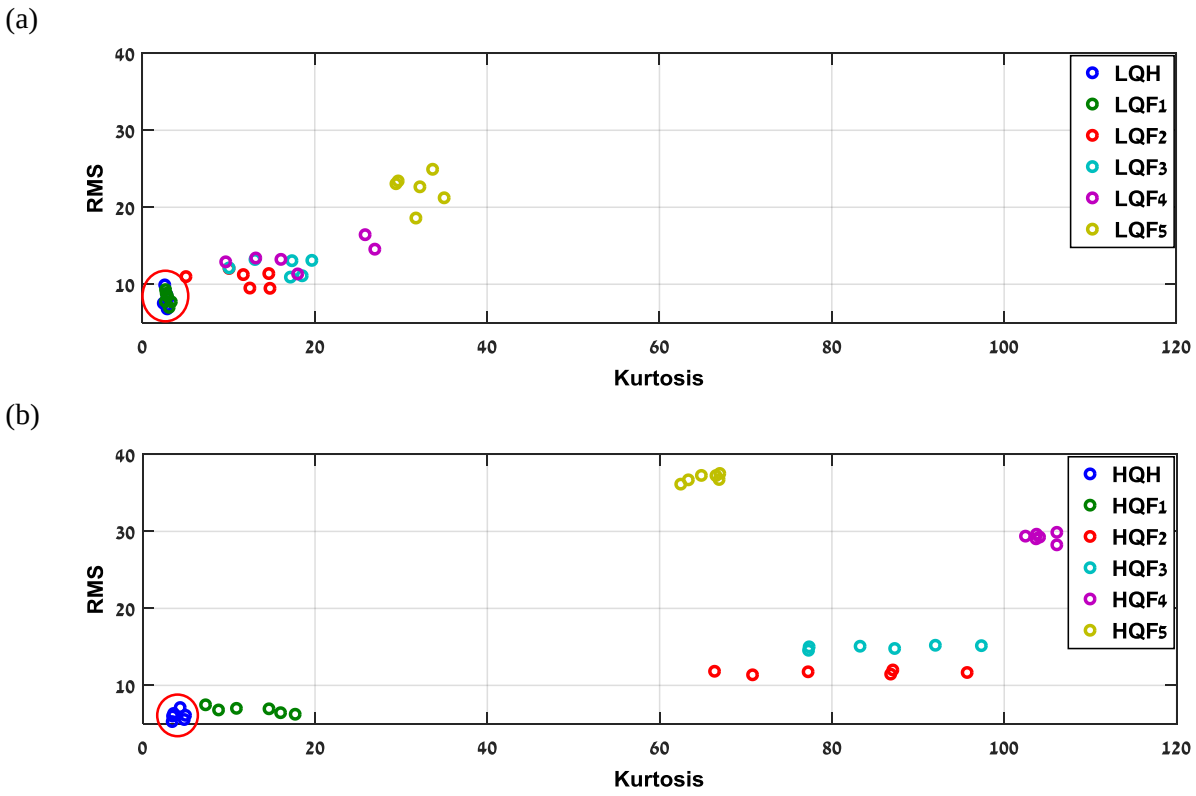

Figure 14: RMS VS Kurtosis - simulated results. (a) low surface quality; (b) high surface quality.

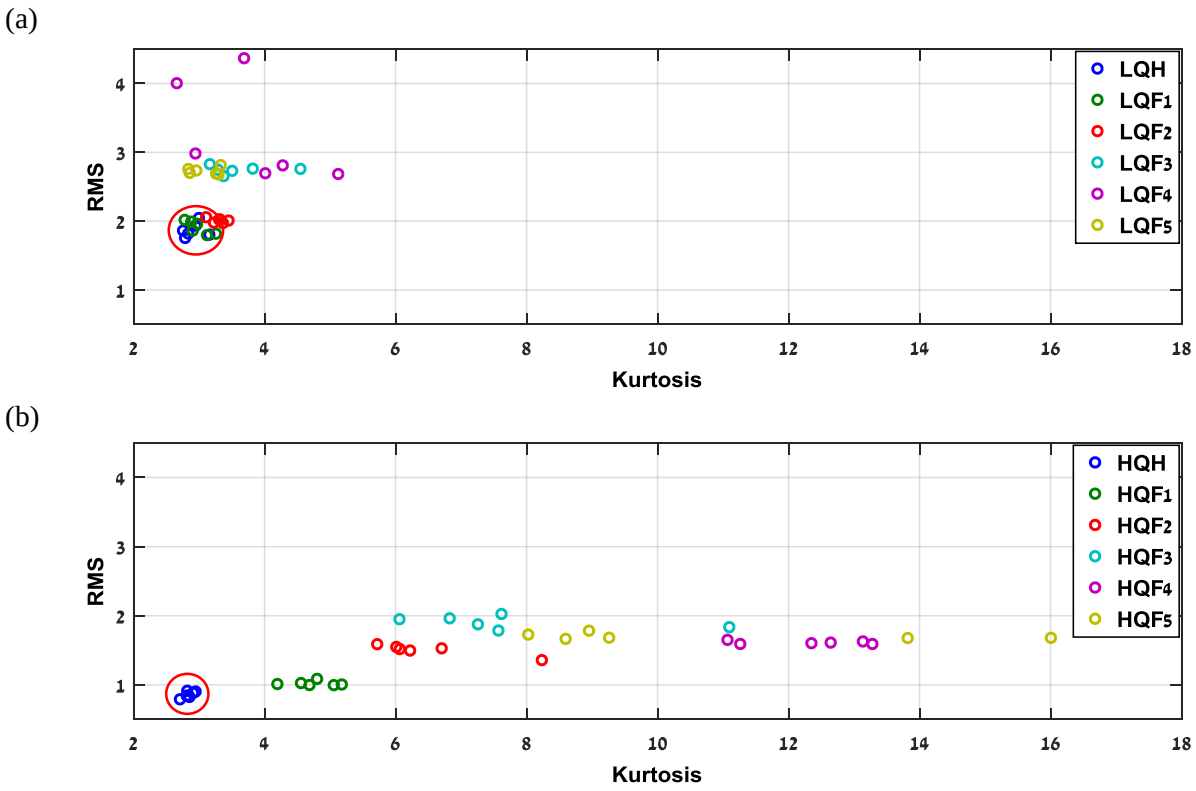

Figure 15: RMS VS Kurtosis - experimental results. (a) low surface quality; (b) high surface quality.

5 Summary and conclusions

The effect of gear tooth surface quality on fault detection capability is examined. A dynamic model was deployed in order to improve the physical understanding of effects of faults. It is used to study the influence of different profile quality levels on the fault detection capability.

Two different gear precision grades with faults of five different levels of severity are simulated and compared with a similar series of experiments.

It is shown that the levels of the profile errors can significantly influence the faults detection capability. It was shown that the model predicts correctly the detectable fault severity for a given teeth surface quality and that gears with high quality teeth surface allow detection of smaller faults. Also, we have shown that meshing of different surface gear teeth of the same precision grade can generate distributed results. The model generated distributions similar to the experimental results.

The model is a powerful tool for assessing diagnostics capabilities and their robustness in a real environment. The number of experiments that can be performed is always limited. The model can be used to extend the number of cases and to obtain a realistic distribution of results allowing a realistic evaluation of diagnostics procedures.

Future research will focus on the effect of additional faults in different types of gear transmission.

Acknowledgments

We gratefully acknowledge the invaluable support of the Pearlstone Foundation.

References

[1]A. Fernández, M. Iglesias, A. de Juan, P. García, R. Sancibrián, F. Viadero, Gear transmission dynamic: Effects of tooth profile deviations and support flexibility, Applied Acoustics 77 (2014) 138–149.

[2]E. Mucchi, G. Dalpiaz, A. Rivola, Elastodynamic analysis of a gear pump. Part II: Meshing phenomena and simulation results, Mechanical Systems and Signal Processing 24 (7) (2010) 2180–2197.

[3]I Dadon, et al. Towards a reliable non-linear dynamic model of damaged gear transmission, Insight-Non-Destructive Testing and Condition Monitoring 57 (5) (2015) 283–289.

[4]American National Standard, Accuracy Classification System – Tangential Measurements for Cylindrical Gears. ANSI AGMA 2015-1-A01 (2002).

[5]Tolerances for Cylindrical Gear Teeth - Tolerances for deviations of individual parameters, DIN 3962-Part 1, Deutsche Normen, Aug. 1978.

[6]H. Endo, R. Randall, C. Gosselin, Differential diagnosis of spall vs. cracks in the gear tooth fillet region: experimental validation, Mechanical Systems and Signal Processing 23 (3) (2009) 636–651.